Quantum scattering calculations for ro-vibrational de-excitation of CO by hydrogen atoms

Lei Song,[1] N. Balakrishnan,[2] Ad van der Avoird,[1] Tijs Karman,[1] and Gerrit C. Groenenboom[1, a)]

[1)] *Theoretical Chemistry, Institute for Molecules and Materials, Radboud University, Heyendaalseweg 135, 6525 AJ Nijmegen, The Netherlands*

[2)] *Department Of Chemistry, University of Nevada-Las Vegas, 4505 Maryland Parkway, Las Vegas, Nevada 89154-4003, USA*

(Dated: May 11, 2015)

We present quantum-mechanical scattering calculations for ro-vibrational relaxation of CO in collision with hydrogen atoms. Collisional cross sections of CO ro-vibrational transitions from $v = 1, j = 0 - 30$ to $v' = 0, j'$ are calculated using the close coupling method for collision energies between 0.1 and 15000 cm^{-1} based on the three-dimensional potential energy surface of Song *et al.* [L. Song, A. van der Avoird, and G.C. Groenenboom, J. Phys. Chem. A, 117, 7571 (2013)]. Cross sections of transitions from $v = 1, j \geq 3$ to $v' = 0, j'$ are reported for the first time at this level of theory. Also calculations by the more approximate coupled states and infinite order sudden methods are performed in order to test the applicability of these methods to H-CO ro-vibrational inelastic scattering. Vibrational de-excitation rate coefficients of CO ($v = 1$) are presented for the temperature range from 100 K to 3000 K and are compared with the available experimental and theoretical data. All of these results and additional rate coefficients reported in a forthcoming paper are important for including the effects of H-CO collisions in astrophysical models.

[a)] Electronic mail: gerritg@theochem.ru.nl

I. INTRODUCTION

Carbon monoxide (CO) is the second most abundant molecule in the universe. Its $\Delta v = 1$ ro-vibrational bands around 4.7 μm are commonly observed in protoplanetary disks using the CRIRES high-resolution infrared spectrometer on the Very Large Telescope (VLT).[1,2] These CO bands now rank among the best tracers of the physical conditions in these disks, thus contributing to the understanding of the gas kinematics. Most analyses of CO ro-vibrational bands assume local thermodynamic equilibrium (LTE). However, more accurate studies of CO emission lines, such as those concerning the efficiency of IR/UV fluorescence, require non-LTE methods.[3] Accurate non-LTE modeling requires reliable collision rate coefficients of CO with its dominant collision partners H, He, and H_2. These rate coefficients can be obtained from scattering calculations based on the interaction potentials of CO with its partners. Besides the accurate close coupling (CC) method, more approximate quantum mechanical approaches such as the coupled states (CS)[4,5] and infinite order sudden (IOS)[6] methods are commonly used for such scattering calculations.

The H-CO collision dynamics has been studied in several experiments[7–9] and calculations.[10–16] Until now, experimental collision rate coefficients are available only for $v = 1 \rightarrow 0$ transitions, without resolution of the transitions between individual rotational levels. The majority of the calculations focus on pure rotational or pure vibrational inelastic collision processes. Progress in ro-vibrational cross section calculations has been slow. The difficulty of reliable H-CO ro-vibrationally inelastic scattering calculations is related to the fact that HCO is a chemically bound species, in contrast with other astrophysically important collision complexes such as He-CO and H_2-CO that are bound only by weak Van der Waals forces. This is illustrated by the depth of the well in the three-dimensional (3D) H-CO potential energy surface (PES) of Song *et al.*[17], which is 0.835 eV (6738 cm^{-1}), whereas He-CO and H_2-CO are bound only by about 23 cm^{-1} and 94 cm^{-1}, respectively[18–21]. Another essential difference with He-CO and H_2-CO important for inelastic collision processes is that the H-CO potential has a barrier for dissociation of HCO into H + CO with a height of 0.141 eV (1138 cm^{-1}) above the H + CO limit, while He-CO and H_2-CO have no barriers. In principle, the strong interaction in H-CO gives rise to strong vibrational coupling and highly efficient translation-vibration (T-V) energy transfer, but in order to get into the region of the deep well the H atom approaching the CO molecule must first pass

over or tunnel through the barrier. As one will see below, this leads to a steep rise of the ro-vibrationally inelastic cross sections when the collision energy surpasses the threshold of 1138 cm^{-1}. When the incoming CO molecule is in a rotationally excited state, it may use some of its rotational energy to help crossing the barrier. This involves rotation-translation (R-T) coupling, which depends sensitively on the anisotropy of the PES in the long range region. Also pure rotationally inelastic cross sections are mostly determined by the long range anisotropy, while the ro-vibrationally inelastic transition cross sections are sensitive to the long and short range anisotropy of the H-CO potential, as well as to its dependence on the CO bond length.

A consequence of these complexities is that in H-CO scattering calculations, a large basis set is required to converge the cross sections. Green *et al.*[13] verified this point in their scattering calculations for ro-vibrational excitation of CO ($v = 0, j = 0$) by H atoms. The convergence of the cross sections was tested in a series of CS calculations at a total energy of 1 eV (8065 cm^{-1}) with basis sets of increasing size. For ro-vibrational transitions to $v' = 1$ and j' values up to 30 as considered in the present paper they found that convergence of the cross sections to within about 10% requires basis sets containing vibration functions up to $v = 8$ and rotation functions up to $j = 90$. Even for qualitative results, converged within a factor of 2, basis sets with two or more vibrational levels above the level of interest should be included. In the full quantum CC approach, the CPU time for the rate-limiting step scales roughly with the third power of the basis size. Therefore, the required large basis sets result in heavy computational efforts. An additional complication was shown by Stepler *et al.*[16] in their CC rigid-rotor calculations for CO ($v = 0, j = 0$) excitation by H atoms based on four different PESs. Their studies revealed that the long-range behavior of the PES strongly affects the inelastic collision cross sections. So it is necessary in the scattering calculations to propagate to a relatively long distance to obtain reliable inelastic cross sections, which increases the computational effort as well.

The incomplete knowledge about ro-vibrational rate coefficients for H-CO collisions obliges astronomers to use scaling laws to fill the gaps. In a recent paper, Thi *et al.*[3] modeled CO ro-vibrational emission from Herbig Ae discs by using extrapolated rate coefficients for H-CO based on the values reported by Balakrishnan *et al.*[22]. In Balakrishnan *et al.*'s work, pure rotational rates were calculated for CO rotational levels up to $j = 7$ for a range of gas temperatures of $5\,\mathrm{K} \leq T \leq 3000\,\mathrm{K}$, while pure vibrational transition rates were

computed in the IOS approximation up to $v = 4$ for a range of gas temperatures of 100 K $\leq T \leq$ 3000 K. The missing rotational rates for j values higher than 7 and vibrational rates below 100 K cause large uncertainties in the extrapolation with the scaling laws. Based on the information from the present paper, we report in a forthcoming paper[23] rate coefficients for ro-vibrational $v = 1, j = 0-30 \rightarrow v' = 0, j'$ and $v = 2, j = 0-30 \rightarrow v' = 1, j'$ transitions and vibrational rates up to $v = 5$ for a range of gas temperatures 10 K $\leq T \leq$ 3000 K. Furthermore, we introduce a new, more reliable method to extrapolate all ro-vibrational transition rates for CO in initial states with $v \leq 5, j \leq 30$.

The accuracy of calculated inelastic cross sections depends strongly on the quality of the PES used. The 3D BBH[24] and WKS[25] potentials were used in scattering calculations in previous work. The BBH potential, however, is insufficiently accurate to reproduce stimulated emission pumping (SEP) spectra.[25,26] This was the reason why Keller *et al.*[25] constructed the WKS potential, but they did not include a sufficiently large number of *ab initio* data points at large H-CO distances to make their potential accurate also in the long range. It was demonstrated by Shepler *et al.*[16] that this seriously affects the accuracy of rotationally inelastic cross sections. The 3D PES of Song *et al.*[17] was constructed with a focus on the long range behavior. In bound state calculations of HCO it reproduces multiple experimental data, which shows that it is accurate also in the well region. In the present work, we adopt this (SAG) potential[17] to calculate state-to-state ro-vibrational de-excitation cross sections for initial states with $v = 1, j = 0-30$ to final states $v' = 0, j'$. In Sec. II we briefly describe the theoretical methods and computational details. The different basis sets and approximation methods are discussed in Sec. III. In the same section we present the calculated ro-vibrational (de-)excitation cross sections and vibrational quenching rate coefficients. Our conclusions follow in Sec. IV.

II. CALCULATIONS

A. Theoretical methods

The Hamiltonian in body-fixed (BF) coordinates for H-CO($\widetilde{X}\,^2A'$) can be written (in atomic units) as

$$\hat{H} = -\frac{1}{2\mu R}\frac{\partial^2}{\partial R^2}R + \frac{\hat{J}^2 + \hat{j}^2 - 2\hat{\boldsymbol{j}}\cdot\hat{\boldsymbol{J}}}{2\mu R^2} + V_{\rm int}(r, R, \theta) + \hat{H}_{\rm CO}, \tag{1}$$

where $\mu = m_{\rm H} m_{\rm CO}/(m_{\rm H} + m_{\rm CO})$ is the reduced mass of the H-CO complex. The vector $\boldsymbol{R}$ with length R, connecting the CO center of mass with the H atom, is embedded along the z axis. The vector $\boldsymbol{r}$, with length r, points from C to O. The angle θ is the angle between the vectors $\boldsymbol{R}$ and $\boldsymbol{r}$. The operator $\hat{\boldsymbol{j}}$ is the rotational angular momentum of the CO molecule, while $\hat{\boldsymbol{J}}$ is the total angular momentum operator of the H-CO complex. The interaction energy between CO and H is written as $V_{\rm int}(r, R, \theta)$. The CO Hamiltonian $\hat{H}_{\rm CO}$ is given by

$$\hat{H}_{\rm CO} = -\frac{1}{2\mu_{\rm CO} r}\frac{\partial^2}{\partial r^2} r + \frac{\hat{j}^2}{2\mu_{\rm CO} r^2} + V_{\rm CO}(r), \tag{2}$$

where $\mu_{\rm CO}$ is the reduced mass of CO and $V_{\rm CO}(r)$ is the potential of free CO.

To solve the time-independent Schrödinger equation with the Hamiltonian of Eq. (1), the wave functions are expanded as

$$\Phi = \frac{1}{R}\sum_{\boldsymbol{n}} |\boldsymbol{n}\rangle\, \psi_{\boldsymbol{n}}(R), \tag{3}$$

where $\psi_{\boldsymbol{n}}(R)$ are functions of the radial coordinate, while the channel basis functions $|\boldsymbol{n}\rangle$ are given by

$$|\boldsymbol{n}\rangle = |v, j, J, K, M\rangle = \left[\frac{2J+1}{4\pi}\right]^{1/2} \frac{1}{r}\chi_{v,j}(r) Y_{j,K}(\theta, \phi) D^{(J)}_{M,K}(\alpha, \beta, 0)^*. \tag{4}$$

They consist of the j-dependent vibrational wave functions $\chi_{v,j}(r)$ of free CO and a BF angular basis set. The spherical harmonics $Y_{j,K}(\theta, \phi)$ and Wigner D-functions $D^{(J)}_{M,K}(\alpha, \beta, 0)^*$ form the angular basis set, in which the angles (θ, ϕ) are the polar angles of the CO axis with respect to the BF frame and the Euler angles $(\alpha, \beta, 0)$ define the orientation of the BF frame with respect to a space-fixed (SF) frame. The quantum numbers v and j label the vibrations and rotations of CO. Other quantum numbers are the total angular momentum J of the H-CO complex and its projections K and M on the BF and SF z-axes, respectively. Angular basis functions with parity $p = (-1)^{J+n}$ symmetrized under inversion are given by

$$\begin{aligned} \frac{1}{\sqrt{2}}\left[Y_{j,K} D^{(J)*}_{M,K} + (-1)^n Y_{j,-K} D^{(J)*}_{M,-K}\right] \qquad & \text{with} \quad n = 0, 1 \qquad \text{for } K > 0 \\ Y_{j,0} D^{(J)*}_{M,0} \qquad & \text{with} \quad n = 0 \qquad \text{for } K = 0. \end{aligned} \tag{5}$$

Substituting the expansion of Eq. (3) into the time-independent Schrödinger equation and projecting with $\langle \boldsymbol{n'}|$ gives the coupled channel equations

$$\frac{\partial^2}{\partial R^2}\psi_{\boldsymbol{n'}}(R) = \sum_{\boldsymbol{n}} \langle \boldsymbol{n'}|\, \hat{W}\, |\boldsymbol{n}\rangle\, \psi_{\boldsymbol{n}}(R). \tag{6}$$

The operator $\hat{W}$ is introduced as

$$\hat{W} = -2\mu \left[E - \hat{H}_{\rm CO} - \frac{\hat{J}^2 + \hat{j}^2 - 2\hat{\boldsymbol{j}} \cdot \hat{\boldsymbol{J}}}{2\mu R^2} - V_{\rm int}(r, R, \theta) \right], \tag{7}$$

where E is the total energy. The eigenvalues of the Hamiltonian $\hat{H}_{\rm CO}$ are the channel energies written as $\epsilon_{v,j}$. The difference $(E - \epsilon_{v,j})$ is the collision energy $E_{v,j}$. Solving the coupled channel equations with the appropriate boundary conditions produces the scattering S matrix, which includes all the information needed to deduce the state-to-state scattering cross sections $\sigma_{v,j\to v',j'}(E_{v,j})$. Computational details are given in Sec. II B. This approach, with the channel basis chosen sufficiently large to converge the solutions of the coupled channel equations, is the accurate close coupling (CC) scattering method used for most calculations in this article. If the off-diagonal part of the Coriolis coupling is neglected, i.e., if the operator $\hat{\boldsymbol{j}} \cdot \hat{\boldsymbol{J}}$ is replaced by $\hat{j}_z \hat{J}_z$ so that K, the eigenvalue of both $\hat{j}_z$ and $\hat{J}_z$, becomes a good quantum number, we obtain the coupled states (CS) approximation. When the exact diagonal Coriolis coupling term is retained, this approach is more accurate than the commonly applied CS approximation[4,5] in which the centrifugal kinetic energy term $(\hat{J}^2 + \hat{j}^2 - 2\hat{\boldsymbol{j}} \cdot \hat{\boldsymbol{J}})/2\mu R^2$ is approximated by a term $L(L+1)/2\mu R^2$ with some effective value of the quantum number L. When using the CS approximation, the matrix $\langle \boldsymbol{n'} | \hat{W} | \boldsymbol{n} \rangle$ becomes block-diagonal, with a block for each K, and the coupled channel equations of Eq. (6) can be separated into subsets for each K to reduce the computational effort. Another method applied in this article is the infinite order sudden (IOS) approximation. In this method, which ignores the rotational energy spacings in comparison with the collision energy[6] and neglects the CO rotational kinetic energy term in the Hamiltonian, it is assumed that the angle θ of the CO molecule remains fixed during the collision. The IOS calculations were performed with the molecular scattering program MOLSCAT[27] to obtain the total vibrational $v = 1 \to v' = 0$ quenching cross section. Coupled channels equations in a pure vibrational basis set are solved in the IOS approximation for a fixed angle θ and the results are averaged over 50 Gauss-Legendre quadrature points θ_i with the proper weights. The basis set includes the lowest 15 vibrational levels, which is sufficient to converge the $v = 1 \to v' = 0$ vibrational transition cross sections.

Rate coefficients for ro-vibrational energy transfer can be obtained by integrating the corresponding state-to-state cross sections over a Boltzmann distribution of collision energies

at a certain temperature T

$$r_{v,j\to v',j'}(T) = \left(\frac{8k_BT}{\pi\mu}\right)^{\frac{1}{2}} \frac{1}{(k_BT)^2} \int_0^\infty \sigma_{v,j\to v',j'}(E_{v,j}) \exp(-\frac{E_{v,j}}{k_BT})\ E_{v,j}\ dE_{v,j}, \tag{8}$$

where k_B is the Boltzmann constant. The state-to-state cross sections $\sigma_{v,j\to v',j'}(E_{v,j})$ can be obtained with the CC method or the CS approximation. The total vibrational quenching cross section from a specific ro-vibrational initial state v, j to final state v' is the sum of cross sections over all final j' states of the v' state, i.e.,

$$\sigma_{v,j\to v'}(E_{v,j}) = \sum_{j'} \sigma_{v,j\to v',j'}(E_{v,j}). \tag{9}$$

The corresponding rate coefficients are written as $r_{v,j\to v'}(T)$. Then, by averaging the rate coefficients over different initial j states, we get the vibrational de-excitation rate coefficients based on the CC method or the CS approximation as follows

$$r_{v\to v'}(T) = \frac{\sum_j g_j \exp(-\frac{\epsilon_{v,j}}{k_BT}) r_{v,j\to v'}(T)}{\sum_j g_j \exp(-\frac{\epsilon_{v,j}}{k_BT})}, \tag{10}$$

where $g_j = 2j + 1$ is the degeneracy of the j rotational level.

B. Computational details

Having described the theoretical formalism, we turn to the numerical details in the calculations of the integral cross sections. The CC and CS calculations were performed with our own scattering codes written in Fortran and Scilab[28], which include some features developed to save computational resources. As usual in scattering calculations, we expand the anisotropic interaction potential $V_{\rm int}(r, R, \theta)$ in Legendre polynomials $P_l(\cos\theta)$ and calculate its matrix elements over the angular basis of Eq. (4) analytically in terms of $3j$-symbols.[6] We prepare the angular integrals and R-dependent angular expansion coefficients of the anisotropic potential in advance and save them on disk. The coupled channel equations are solved with the renormalized Numerov propagator[29,30]. During the propagation, instead of keeping the W-matrices in core, our program recomputes the W-matrix from the prepared angular integrals and potential expansion coefficients for every R point, which considerably saves memory. The rate-limiting steps are matrix multiplications and inversions in the renormalized Numerov algorithm; these are run on several cores in parallel with optimized MKL LAPACK library routines. Also the fact that the expression for the W-matrix

elements of the potential becomes simpler in the BF angular basis than in the usual space-fixed (SF) basis saves both computer time and storage. Moreover, when applying the CS approximation, we divide the problem into smaller blocks for each K quantum number. At the end of the propagation, the radial solutions $\psi_{\boldsymbol{n}}(R)$ associated with the BF angular basis $|\boldsymbol{n}\rangle = |v, j, J, K, M\rangle$ are transformed into the corresponding ones for the SF basis $|v, j, L, J, M\rangle$ with the end-over-end rotational quantum number L, in order to apply the scattering boundary conditions formulated in the SF frame. The exact solution of the space-fixed scattering Schrödinger equation at the outer boundary where the interaction energy $V_{\rm int}(r, R, \theta)$ has vanished, is a linear combination of spherical Bessel functions labeled with the quantum number L. The matching of the propagated radial wave functions to spherical Bessel functions was carried out at the boundary $R_{\rm max}$ with values of 40 to 18 a_0 adapted to a range of collision energies from $E_{v,j} = 0.1$ to 15000 cm^{-1}. The propagation step size varied from 0.032 to 0.055 a_0. The parallellization and memory saving features of the code reduce the requirement on the computational resources dramatically, which made it possible to use hundreds of simple personal computers connected over a regular ethernet network for a large number of small jobs.

As usual in scattering calculations, we exploit the property that J, M, and the parity p are good quantum numbers and we collect the corresponding contributions to the integral cross sections from separate calculations. The maximum value of J needed to converge the cross sections depends on the collision energy and the initial j value; values of J up to 100 were used. Using the CC method, we calculated the state-to-state de-excitation cross sections from $v = 1, j = 0 - 30$ to $v' = 0, j'$. Initially we adopted two basis sets $B3(61, 52, 40, 22)$ and $B9(79, 70, 59, 45, 45, 30, 30, 25, 25, 25)$ for the calculations with initial states $v = 1, j = 0 - 10$, where the notation $Bn(j_0, j_1, j_2, ..., j_n)$ indicates a basis with the highest vibrational level n and the highest rotational level j_i included for vibrational level $v = i$. We notice in Table I that the number of channels in the $B9$ and $B3$ basis sets increases dramatically with increasing J. The number of channels for $B3$ is less than half of that for the $B9$ basis. The third power of the ratio of the numbers of channels for $B9$ and $B3$ is around 15 to 18, which implies that the calculation with the $B3$ basis is 15-18 times faster than the one with the $B9$ basis. To further reduce the computational effort, we adapted the renormalized Numerov algorithm so that we could gradually omit closed channels during the propagation.[31] This saved about 30% of CPU time and did not

deteriorate the accuracy of the results by more than 0.001%. This truncation is based on the idea that the coupling with higher energy levels diminishes when the potential becomes smaller for larger R. The criterion used to truncate the channel basis considers the channel energies and is an exponential function of R dependent on the decay of the potential with increasing R. The accuracy of the CS approximation is tested by comparison with full CC calculations performed for the initial states $v = 1, j = 0 - 10$ with basis $B3(61, 52, 40, 22)$. The propagation was done separately for the different K blocks of the W-matrix and the propagated results for all K with $-J \leq K \leq J$ were combined and transformed to the SF basis when applying the L-dependent outer boundary conditions.

III. RESULTS AND DISCUSSION

A. Convergence test

By comparison with the results from an even larger basis set $B9^*(84, 75, 64, 50, 50, 35, 35, 30, 30, 30)$ we could show that the $B9(79, 70, 59, 45, 45, 30, 30, 25, 25, 25)$ basis yields cross sections of the transitions $v = 1, j = 0 - 10 \rightarrow v' = 0, j'$ converged to within 10% at collision energies $E_{v,j} \leq 5000$ cm^{-1}, which is in agreement with the results of convergence tests by Green *et al.*[13]. An accuracy of 10% is sufficient for the applications in astronomy that we are aiming at. Even our $B9$ basis is still large, however, and produces up to 11,000 scattering channels. In order to reduce our computational efforts, we tested a smaller $B3(61, 52, 40, 22)$ basis set for initial states with $v = 1, j = 0 - 10$. Figure 1 shows that the state-to-state cross sections from the $B9$ and $B3$ bases are similar, except that some fine resonance structures are lost with the $B3$ basis set which may affect the rate coefficients. The root mean square relative difference of the rate coefficients from the two bases is less than 25%, which makes the values from the $B3$ basis sufficiently accurate for applications in astronomy. In addition, since resonances become less important with increasing initial rotational quantum number j —which will be illustrated in Sec. III C— use of the smaller basis is expected to have a much smaller influence on the rate coefficients for the transitions from initial $v = 1$ states with $j > 10$. Our final choice was to employ a $B4(70, 60, 49, 36, 15)$ basis for the transitions from $v = 1, j = 11 - 30$ and the $B9(79, 70, 59, 45, 45, 30, 30, 25, 25, 25)$ basis for transitions from states with lower initial j values. Table 1 shows that the use of CPU time with the

$B4(70, 60, 49, 36, 15)$ basis is 6 or 7 times less than with the $B9$ basis.

B. Tests of the CS and IOS approximations

One of the options to calculate cross sections more efficiently is the CS approximation. To test its accuracy, we performed scattering calculations for initial states $v = 1, j = 0-10$ with the $B3(61, 52, 40, 22)$ basis. Figure 2 shows a comparison of total quenching cross sections from $v = 1, j = 0, 5, 10$ to $v' = 0$ based on the CC method and the CS approximation. The total quenching cross sections are obtained by summation of the state-to-state cross sections over all final rotational states, see Eq. (9). In comparison with the accurate CC calculations, the CS approximation produces reliable cross sections for collision energies above 1000 cm^{-1}. The deviation of the CS cross sections from the CC results at lower energies becomes larger for higher quantum numbers j. The CS approximation is obtained from the CC method by neglecting the off-diagonal Coriolis coupling terms in the kinetic energy operator. The terms neglected are more or less proportional to $\sqrt{j(j+1)}$, which explains why the CS approximation becomes worse with increasing j. So, we must conclude that the CS approximation is not suitable for the calculation of the H-CO ro-vibrational de-excitation rates. The CS approximation has the tendency to perform well for processes dominated by short-range repulsive interactions; in the present study of H-CO we do not find ourselves in that situation, however. In the top panel of Fig. 2, we also present the cross section for vibrational $v = 1 \rightarrow v' = 0$ transitions based on the IOS approximation. The IOS results for this transition agrees fairly well with the CC values for $v = 1, j = 0 \rightarrow v' = 0$ quenching. They also agree well with the total vibrational $v = 1 \rightarrow v' = 0$ quenching cross section from CC calculations obtained by averaging the $v = 1, j \rightarrow v' = 0$ cross sections over initial j levels, see Eq. (10). The latter are not explicitly shown in Fig. 2, but one can observe in this figure that the $v = 1, j = 0 \rightarrow v' = 0$ cross sections hardly depend on the initial j values —apart from resonance structures, which are most pronounced for $j = 0$—, so that the averaging over j has only a minor effect.

C. Cross sections

Examples of energy dependent state-to-state integral cross sections of the transitions from initial states $v = 1, j = 0, 10, 15, 25$ to individual final states $v' = 0, j' = 0, 5, 10, 15, 20$ are shown in Fig. 3. One observes in this figure that the cross sections from the same initial v, j states have a similar energy dependence. Figure 3(a) shows that the cross sections from initial state $v = 1, j = 0$ have abundant structures, due to resonances. Panels (b), (c), and (d) of this figure illustrate that these structures vanish with increasing initial j.

All of these state-to-state cross sections are relatively small for low collision energy, stay more or less constant with increasing energy, and then increase by three orders of magnitude at energies in the range from 100 to 1000 cm^{-1}, followed by a flatter behavior in the high energy region. The increase of the cross sections is steepest for the initial CO state with $j = 0$, where it starts at collision energies around 1000 cm^{-1}. The explanation of this dramatic increase is the existence of a barrier with a height of 1138 cm^{-1} in the entrance channel of the H-CO potential surface. Vibration-translation (V-T) and vibration-rotation (V-R) energy transfer mainly takes place at short H-CO distances in the chemical bonding and repulsive region of the H-CO potential, inside of the barrier, where the potential depends most sensitively on the CO bond length. For higher initial rotational quantum number j of CO the increase of the cross sections becomes more gradual and starts at lower collision energy. This can be explained by a release of the initial rotational energy of CO through rotation-translation (R-T) energy transfer when the system approaches the barrier. The additional translational energy helps the system to overcome the barrier, so that this can happen at lower collision energies. R-T energy transfer is caused by anisotropic H-CO interactions, which makes it important that the long range anisotropy of the potential is accurate. This interplay of short and long range interactions in H-CO leads to a much more complex behavior than in a weakly bound system as He-CO, where ro-vibrational energy transfer processes[32] are all determined by van der Waals interactions. Due to this dramatic increase of the cross sections at collision energies of about 1000 cm^{-1}, their high-energy contribution to the rate coefficients is much more important than usual. Therefore, cross sections at relatively high energies needed to be computed and included in the calculation of the H-CO rate coefficients by Boltzmann averaging over collision energies, even for lower temperatures. This is another reason why the calculation of rate coefficients for H-CO

collisions is so expensive.

In Fig. 4 we present the total quenching cross sections from initial states $v = 1, j = 1, 8, 15, 20, 30$ to final $v' = 0$. The general behavior of these cross sections is similar to that of the state-to-state cross sections, but the structures in the cross sections are washed out to some extent in the sum of state-to-state cross sections over all final j' values. Apart from resonances, the cross sections from higher initial j states are always larger at collision energies below 1000 cm^{-1}. For higher energies the total quenching cross sections for different initial j values become almost equal and gently rise together.

The contributions from individual partial waves to the total quenching cross sections are shown in Fig. 5 for four different initial states with $j = 0$, 10, 20, and 30. In the top panel, for a collision energy of 0.1 cm^{-1}, the contributions are all sharply peaked with maxima appearing at $J = j$. This reveals the dominant contribution of s-wave ($L = 0$) scattering at this low energy. For a collision energy of 5000 cm^{-1} the contributions from different total J values are much more broadly distributed, as illustrated in the bottom panel of the figure. For the higher initial j values of 20 and 30, the maxima still correspond to $J = j - 1$ or j , while for lower initial j values of 0 and 10, they appear at J values higher than j. The higher the collision energy, the larger the number of partial waves needed to obtain converged cross sections. Moreover, the contributions from different partial waves shift to higher J for higher initial j. For both reasons the number and size of the computations increase dramatically for higher collision energy.

The distributions of the final rotational levels j' in ro-vibrationally inelastic $v = 1, j \rightarrow v' = 0, j'$ collisions with collision energies $E_{v,j} = 0.1$ cm^{-1} and 5000 cm^{-1} are presented in Fig. 6. At the low collision energy, the final rotational level distributions are dominated by $\Delta j = 0$ transitions for initial j values of 0 and 10. For the higher initial j values they become broader. At the higher collision energy, the distributions of the final rotational levels j' are broader for all initial j values, but they still show maxima for $\Delta j = 0$ transitions for the higher initial j values of 20 and 30. At both collision energies one observes oscillations in the j' distributions which are due to the competition of rotationally inelastic processes induced by the terms with even and odd l in the Legendre expansion of the anisotropic H-CO interaction potential. This explanation is basically the same as the explanation given for the propensity of even/odd Δj transitions in the $v = 0$ ground state[17], but the nature of the oscillations becomes less simple when vibrational inelasticity is involved.

D. Vibrational quenching rate coefficients

The vibrational $v = 1 \rightarrow v' = 0$ quenching rate coefficients of CO in collisions with H atoms can be calculated directly from the IOS approximation, but can also be obtained from state-to-state cross sections calculated with the CC method through the use of Eqs. (8), (9), and (10). In Fig. 7 we plot these rates in the temperature range from 100 K to 3000 K. The CC results are plotted as a green line with cross markers, the IOS values calculated from the same (SAG) H-CO potential of Song *et al.* are shown in the figure as a dark red dashed line. The difference between the CC and IOS rate coefficients is small, which implies that the IOS method is a good approximation for the calculation of pure vibrational de-excitation rate coefficients. The results of IOS calculations of Balakrishnana *et al.*[22] on the semi-empirically adjusted WKS potential are slightly larger than our values from the SAG potential at temperatures below 1500 K. This is a consequence of the dissociation barrier of HCO to H + CO on the modified WKS potential being somewhat lower than on the SAG potential. In Fig. 7 we also plot experimental results measured by Glass *et al.*[8] and by von Rosenberg *et al.*[7]. The solid lines with square and circular markers are fits to the measured data, while the dashed lines are extrapolations of these fits to temperatures not accessed by the measurements. Other dashed lines in Fig. 7 illustrate some empirical formulas used by astronomers.[33,34] The differences between the experimental data from Refs. 7 and 8 are large. Von Rosenberg *et al.*[7] only speculated on the occurrence of H-CO collisions affecting their measurements for other species, and they estimated the effect of collisions with hydrogen atoms on the CO relaxation. Glass *et al.*[8] performed H-CO scattering experiments at various temperatures and pressures, so we believe that their data are more reliable. Our CC and IOS vibrational quenching coefficient rates agree well with these data[8], which implies that the 3D SAG potential is suitable for the calculation of vibrational quenching rate coefficients. The IOS calculations on the modified WKS potential reproduce the experimental data as well, which indicates that the vibrational energy is released in the well region where the two potential surfaces are similar and that the vibrational quenching rate coefficients are less sensitive to the long range part of the potential. However, as mentioned in previous publications[16,35] and also here, the modified WKS potential is less successful in predicting rotationally inelastic scattering cross sections, owing to its less accurate long range part, and this will probably hold also for the state-to-state ro-vibrational cross sections and rate

coefficients.

IV. CONCLUSIONS

State-to-state ro-vibrational $v, j \rightarrow v', j'$ transition cross sections for CO in collision with H atoms are obtained by means of the full close coupling (CC) method with the 3D (SAG) potential of Song *et al.*[17]. Ro-vibrational basis sets with maximum v and j values of 9 and 79, respectively, and up to 11,000 channels are required to converge the ro-vibrational transition cross sections and corresponding rate coefficients to a level appropriate for astronomical applications. Comparison with results obtained from coupled-states (CS) calculations shows that the CS approach is less suitable in this case. Pure vibrational $v \rightarrow v'$ transition cross sections and rate coefficients are obtained from the CC results by summation over final rotational levels j' and averaging over initial levels j and they were computed also in the infinite order sudden (IOS) approximation. The CC and IOS results are in good agreement, which shows that the IOS method works well for $v \rightarrow v'$ transitions. The computed $v \rightarrow v'$ rate coefficients also agree with the measured data of Glass *et al.*[8].

We find, in agreement with earlier work[16], that pure rotational $j \rightarrow j'$ transition cross sections are mainly sensitive to the anisotropy of the H-CO potential in the long range. Ro-vibrational transitions require the system to enter the short range region, where the H-CO potential has a deep well ($D_e = 6738$ cm^{-1}) at a H-CO distance of 3.021 a_0 and the coupling to the CO vibration is most effective. A barrier of 1138 cm^{-1} is present in the H+CO entrance channel, however, which explains why the calculated $v, j \rightarrow v', j'$ cross sections increase by three orders of magnitude when the collision energy surpasses 1000 cm^{-1}. Overcoming the barrier is facilitated through R-T energy transfer when CO is initially in a higher rotational level j; we observe that the rise of the $v, j \rightarrow v', j'$ cross sections starts at lower collision energies and becomes less steep in that case. Both the anisotropy of the H-CO potential and its dependence on the CO bond length are important for these combined processes, and this also explains why such large basis sets are needed to converge the ro-vibrationally inelastic cross sections.

In a forthcoming paper[23] we present ro-vibrational transition rate coefficients for CO in collision with H atoms for transition rate coefficients for CO in collision with H atoms for temperatures up to 3000 K. The dramatic rise of the $v, j \rightarrow v', j'$ cross sections when

the collision energy gets above 1000 cm^{-1} made it necessary to sample a relatively large set of high collision energies in the Boltzmann averaging, even for lower temperatures. In combination with the large basis sets required, this made the calculations computationally very demanding. We described some special features of our close-coupling scattering code that facilitated the computations.

Acknowledgements

The work is supported by The Netherlands Organisation for Scientific Research, NWO, through the Dutch Astrochemistry Network, and in part by the National Science Foundation under Grant No. NSF PHY11-25915. N. B. is supported in part by NSF grant PHY-1205838. We gratefully acknowledge the computer and communication department (C&CZ) of the Faculty of Science of the Radboud University Nijmegen for computer resources and technical support.

REFERENCES

[1]K. Pontoppidan, G. Blake, E. van Dishoeck, A. Smette, M. Ireland, and J. Brown, Astrophys. J. **684**, 1323 (2008).

[2]G. van der Plas, M. van den Ancker, B. Acke, A. Carmona, C. Dominik, D. Fedele, and L. Waters, Astron. Astrophys. **500**, 1137 (2009).

[3]W. F. Thi, I. Kamp, P. Woitke, G. van der Plas, R. Bertelsen, and L. Wiesenfeld, Astron. Astrophys. **551**, A49 (2013).

[4]P. McGuire and D. J. Kouri, J. Chem. Phys. **60**, 2488 (1974).

[5]R. T. Pack, J. Chem. Phys. **60**, 633 (1974).

[6]W. A. Lester, "The n coupled-channel problem," in *Dynamics of molecular collisions, Part A*, edited by W. H. Miller (Plenum, New York, 1976) pp. 1–32.

[7]C. W. von Rosenberg Jr., R. L. Taylor, and J. D. Teare, J. Chem. Phys. **54**, 1974 (1971).

[8]G. P. Glass and S. Klronde, J. Phys. Chem. **86**, 908 (1982).

[9]P. V. Kozlov, V. N. Makarov, V. A. Pavlov, and O. P. Shatalov, Shock Waves **10**, 191 (2000).

[10]S.-I. Chu and A. Dalgarno, R. Soc. London Proc. Ser. A **342**, 191 (1975).

[11]H.-J. Werner, C. Bauer, P. Rosmus, H.-M. Keller, M. Stumpf, and R. Schinke, J. Chem. Phys. **102**, 3593 (1995).

[12]H.-M. Keller, H. Floethmann, A. J. Dobbyn, R. Schinke, H.-J. Werner, C. Bauer, and P. Rosmus, J. Chem. Phys. **105**, 4983 (1996).

[13]S. Green, B. Pan, and J. M. Bowman, J. Chem. Phys. **102**, 8800 (1995).

[14]S. Green, H.-M. Keller, R. Schinke, and H.-J. Werner, J. Chem. Phys. **105**, 5416 (1996).

[15]B. Yang, P. C. Stancil, and N. Balakrishnan, J. Chem. Phys. **123**, 094308 (2005).

[16]B. C. Shepler, B. H. Yang, T. J. Dhilip Kumar, P. C. Stancil, J. M. Bowman, N. Balakrishnan, P. Zhang, E. Bodo, and A. Dalgarno, Astron. Astrophys. **475**, L15 (2007).

[17]L. Song, A. van der Avoird, and G. C. Groenenboom, J. Phys. Chem. A **117**, 7571 (2013).

[18]T. G. A. Heijmen, R. Moszynski, P. E. S. Wormer, and A. van der Avoird, J. Chem. Phys. **107**, 9921 (1997).

[19]K. A. Peterson and G. C. A. McBane, J. Chem. Phys. **124**, 229901 (2006).

[20]P. Jankowski, A. R. W. McKellar, and K. Szalewicz, Science **336**, 1147 (2012).

[21]P. Jankowski, L. A. Surin, A. Potapov, S. Schlemmer, A. R. W. McKellar, and K. Szalewicz, J. Chem. Phys. **138**, 084307 (2013).

[22]N. Balakrishnan, M. Yan, and A. Dalgarno, Astrophys. J. **568**, 443 (2002).

[23]L. Song, N. Balakrishnan, K. Walker, P. C. Stancil, A. van der Avoird, and G. C. Groenenboom, , in preparation (2015).

[24]J. M. Bowman, J. S. Bittman, and L. B. Harding, J. Chem. Phys. **85**, 911 (2013).

[25]H.-M. Keller, H. Floethmann, A. J. Dobbyn, R. Schinke, H.-J. Werner, C. Bauer, and P. Rosmus, J. Chem. Phys. **105**, 4983 (1996).

[26]J. D. Tobiason, J. R. Dunlop, and E. A. Rohlfing, J. Chem. Phys. **103**, 1448 (1995).

[27]J. M. Hutson and S. Green, MOLSCAT computer code, version 14 (1994), distributed by Collaborative Computational Project No. 6 of the Engineering and Physical Sciences Research Council (UK).

[28]Scilab Enterprises, *Scilab: Free and Open Source software for numerical computation*, Scilab Enterprises, Orsay, France (2012).

[29]B. R. Johnson, J. Chem. Phys. **69**, 4678 (1978).

[30]B. R. Johnson, NRCC Proceedings **5**, 86 (1979).

[31]R. Martinazzo, E. Bodo, and F. Gianturco, Comp. Phys. Com. **151**, 187 (2003).

[32]R. V. Krems, J. Chem. Phys. **116**, 4517 (2002).

[33]D. A. Neufeld and D. J. Hollenbach, Astrophys. J. **428**, 170 (1994).

[34]D. Hollenbach and C. F. McKee, Astrophys. J. Suppl. Ser. **41**, 555 (1979).

[35]B. Yang, P. C. Stancil, N. Balakrishnan, R. C. Forrey, and J. M. Bowman, Astrophys. J. **771**, 49 (2013).

Table I. Number of channels with the $B3$, $B4$, and $B9$ basis sets for total $J = 0$ (parity $p = 1$) and $J = 5, 10, 20, 50, 80$ (parity $p = -1$).

J	$B3$	$B4$	$B9$	$\left(\frac{B9}{B3}\right)^3$	$\left(\frac{B9}{B4}\right)^3$
0	179	235	443	15	7
5	1014	1335	2508	15	7
10	1570	2075	3880	15	7
20	2740	3660	6760	15	6
50	4273	6061	10700	16	6
80	4342	6326	11390	18	6

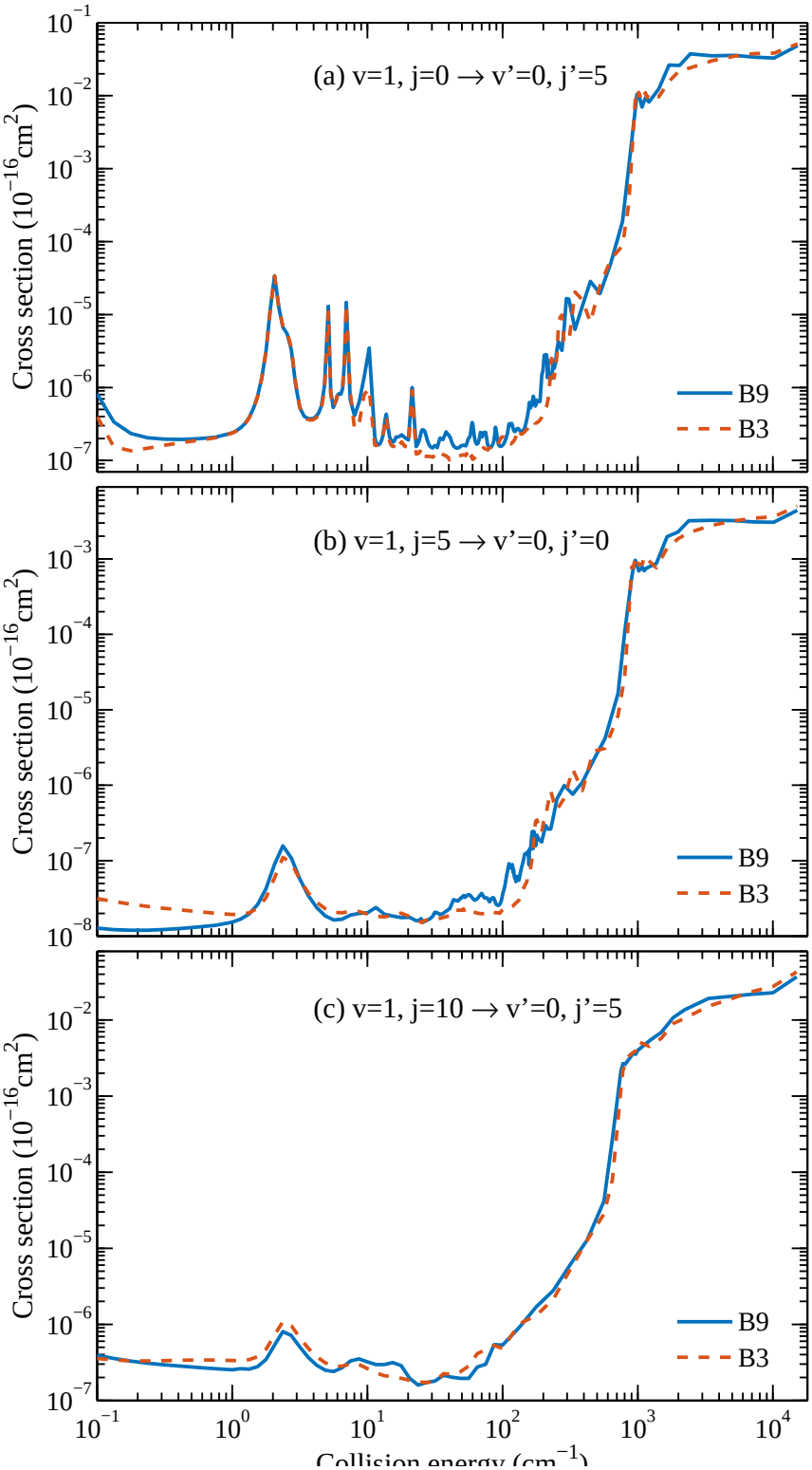

Figure 1. Comparison of state-to-state cross sections for H+CO calculated with the $B9(79, 70, 59, 45, 45, 30, 30, 25, 25, 25)$ and $B3(61, 52, 40, 22)$ basis sets.

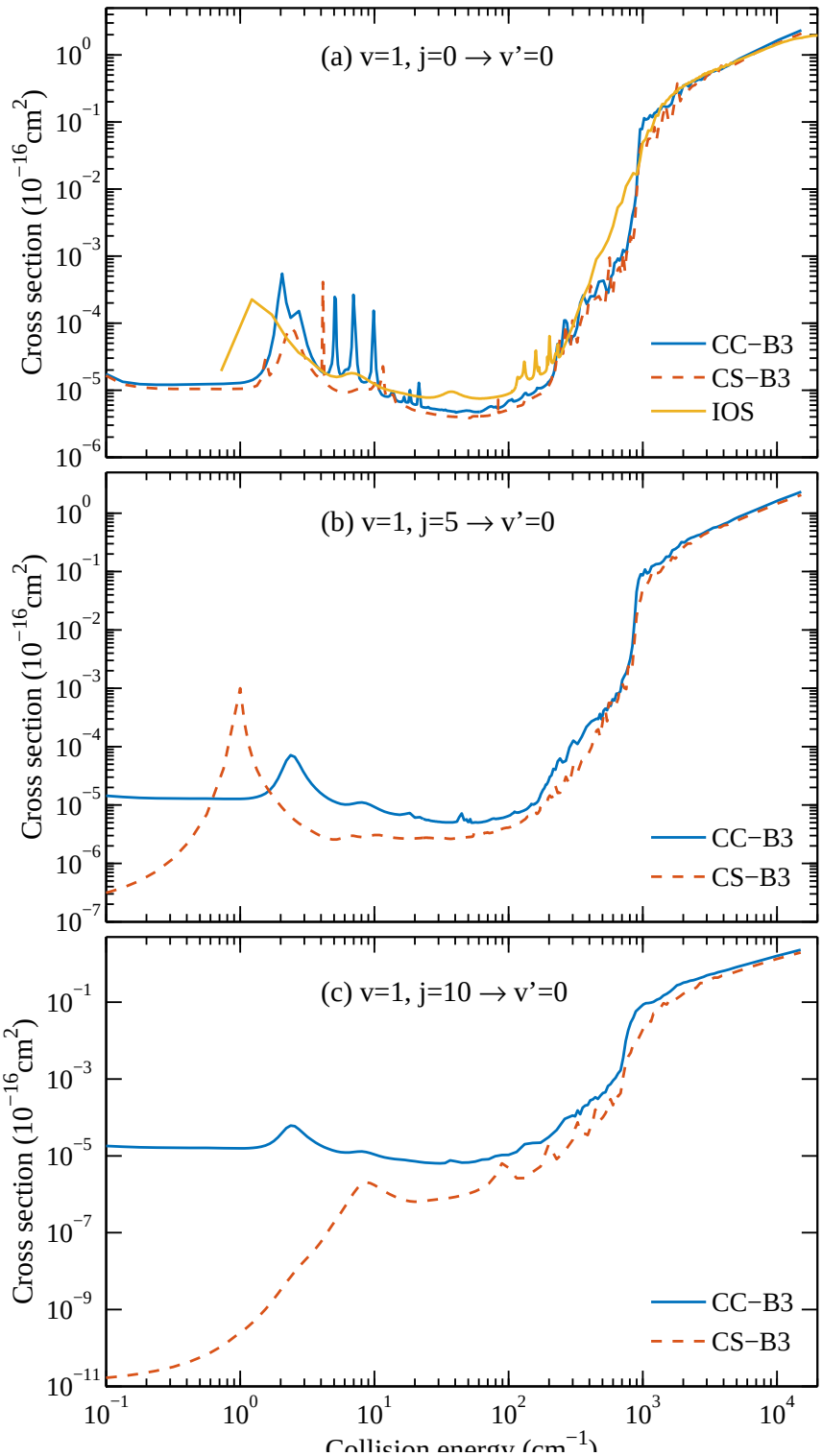

Figure 2. Comparison of total quenching cross sections for H+CO based on the accurate close coupling method, the coupled states approximation, and the infinite order sudden approximation. The line labeled "IOS" shows the cross sections of the vibrational $v = 1 \rightarrow v' = 0$ transition from the IOS approximation.

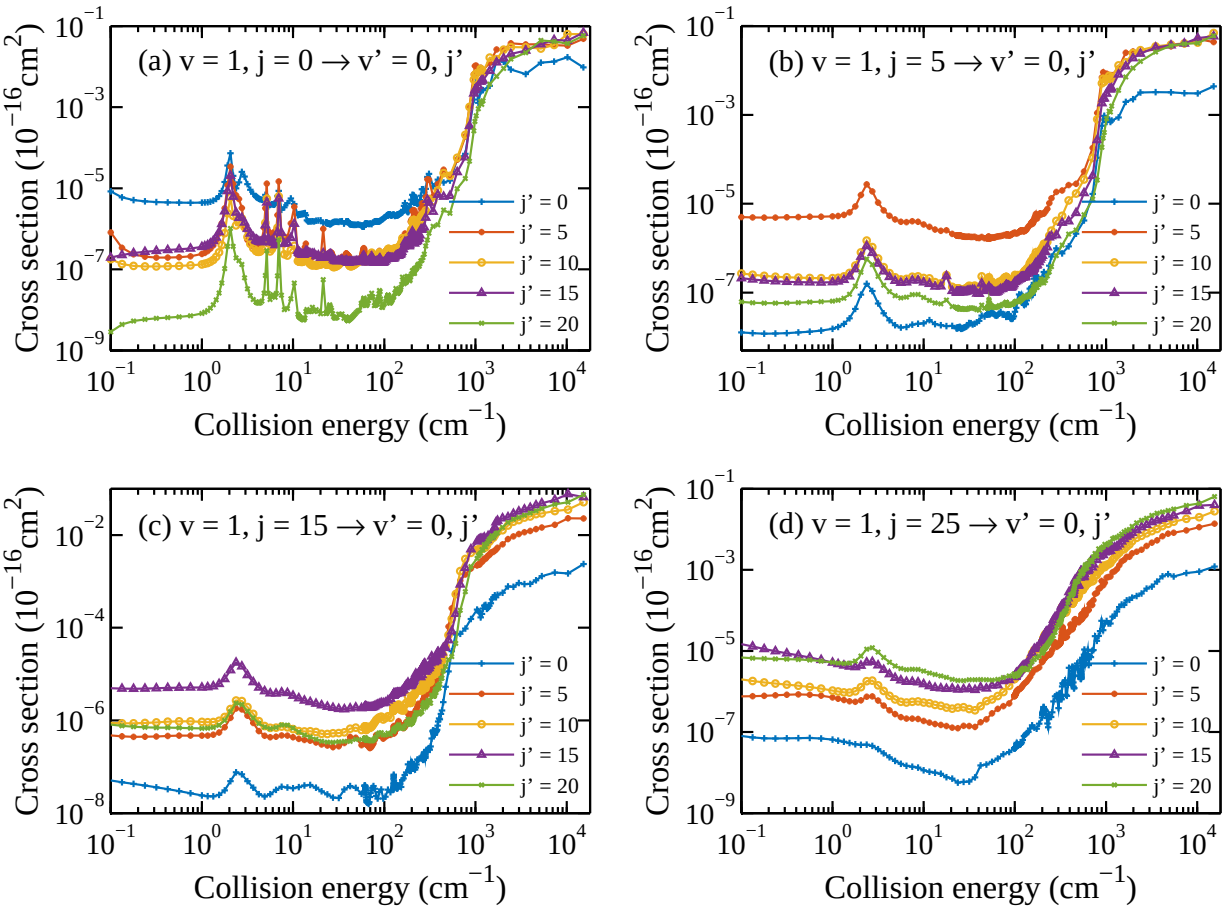

Figure 3. State-to-state cross sections of CO in collision with H atoms from initial states $v = 1, j = 0, 10, 15, 25$ to individual final states $v' = 0, j' = 0, 5, 10, 15, 20$. For initial states $v = 1, j = 0, 10$ the values are calculated with the $B9(79, 70, 59, 45, 45, 30, 30, 25, 25, 25)$ basis.

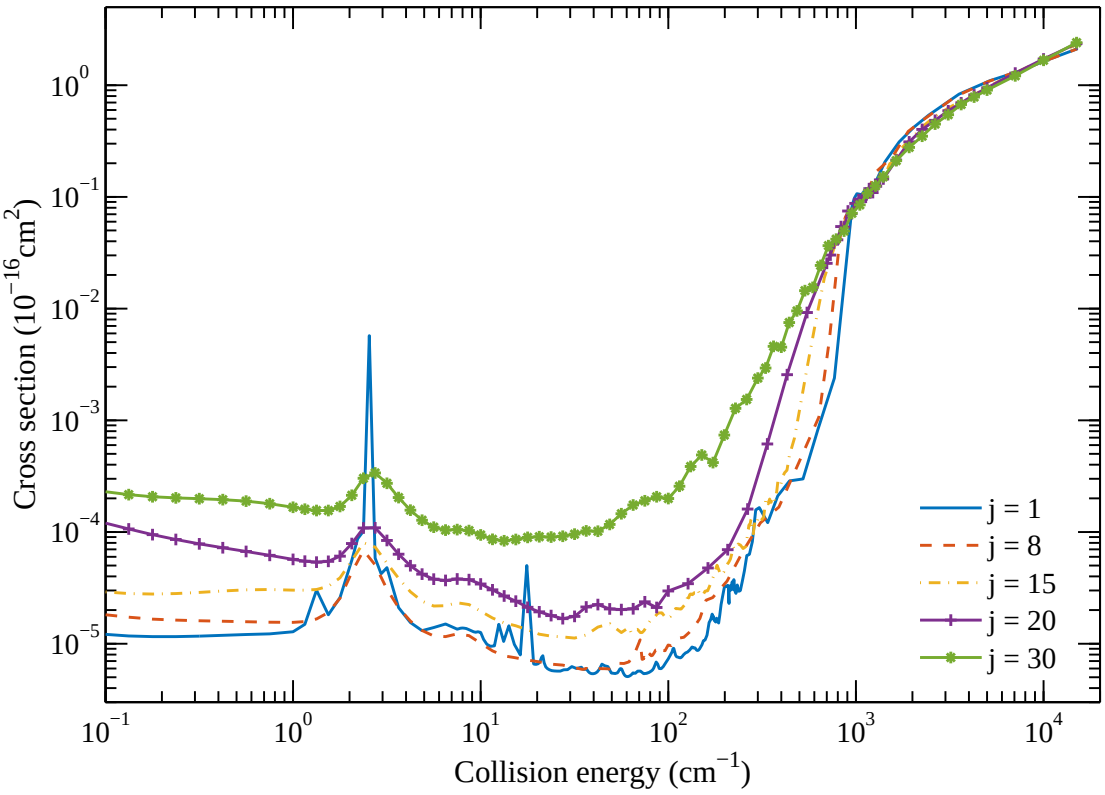

Figure 4. Total quenching cross sections of CO in collision with H atoms from $v = 1, j = 1, 8, 15, 20, 30$ to $v' = 0$. For initial states $v = 1, j = 0, 8$, the values are calculated with the $B9(79, 70, 59, 45, 45, 30, 30, 25, 25, 25)$ basis.

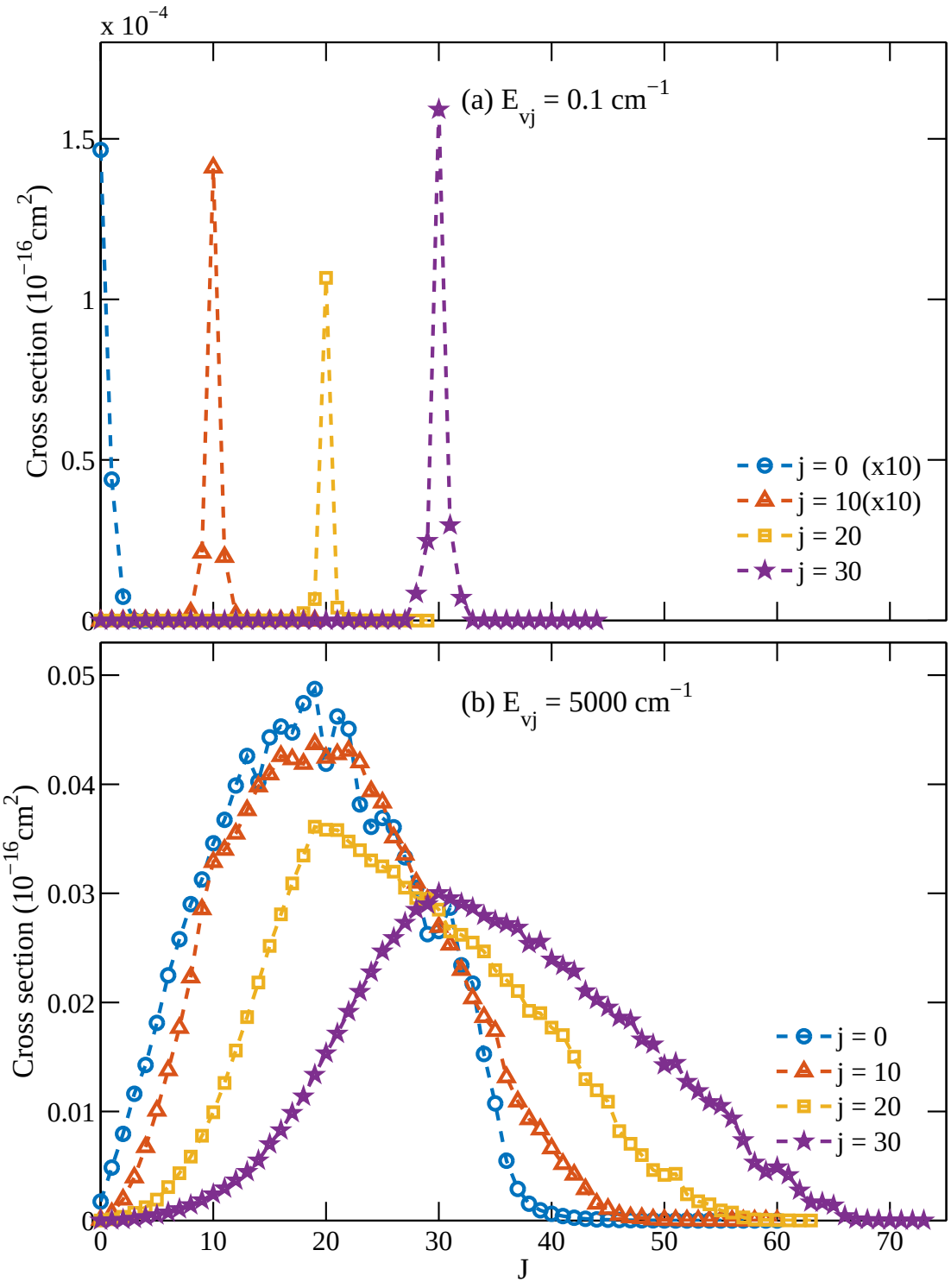

Figure 5. Contributions to the total quenching cross sections for H+CO from different total angular momenta J for the transitions from $v = 1, j = 0, 10, 20, 30$ to $v' = 0$ at collision energies (a) $E_{v,j}$ = 0.1 cm^{-1} and (b) $E_{v,j}$ = 5000 cm^{-1} (5210 cm^{-1} for $j = 0$).

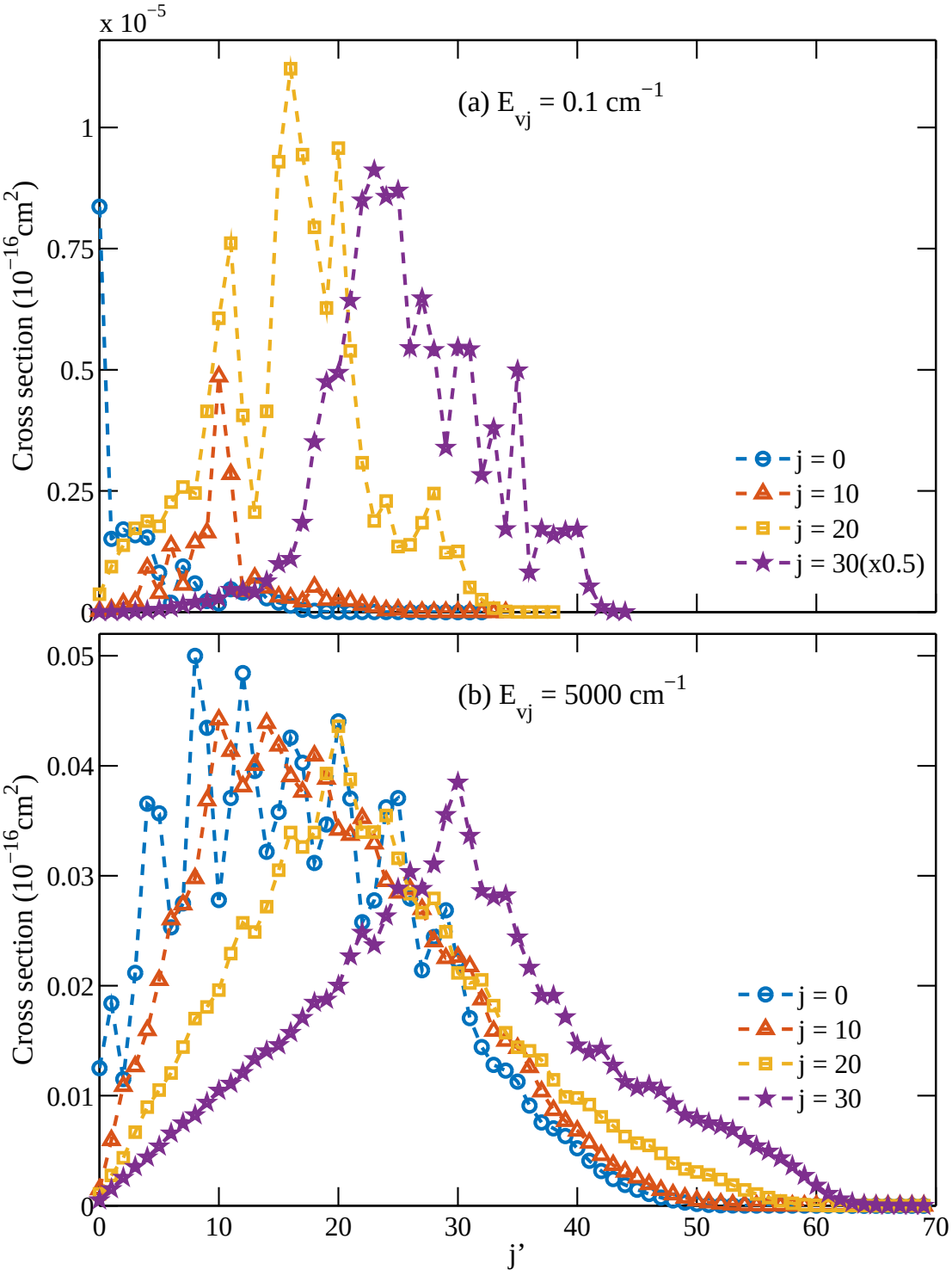

Figure 6. Distributions of final rotational levels j' in the $v' = 0$ vibrational level from de-excitation of initial states $v = 1, j = 0, 10, 20, 30$ at collision energies (a) $E_{v,j} = 0.1$ cm^{-1} and (b) $E_{v,j} = 5000$ cm^{-1} (5210 cm^{-1} for $j = 0$).

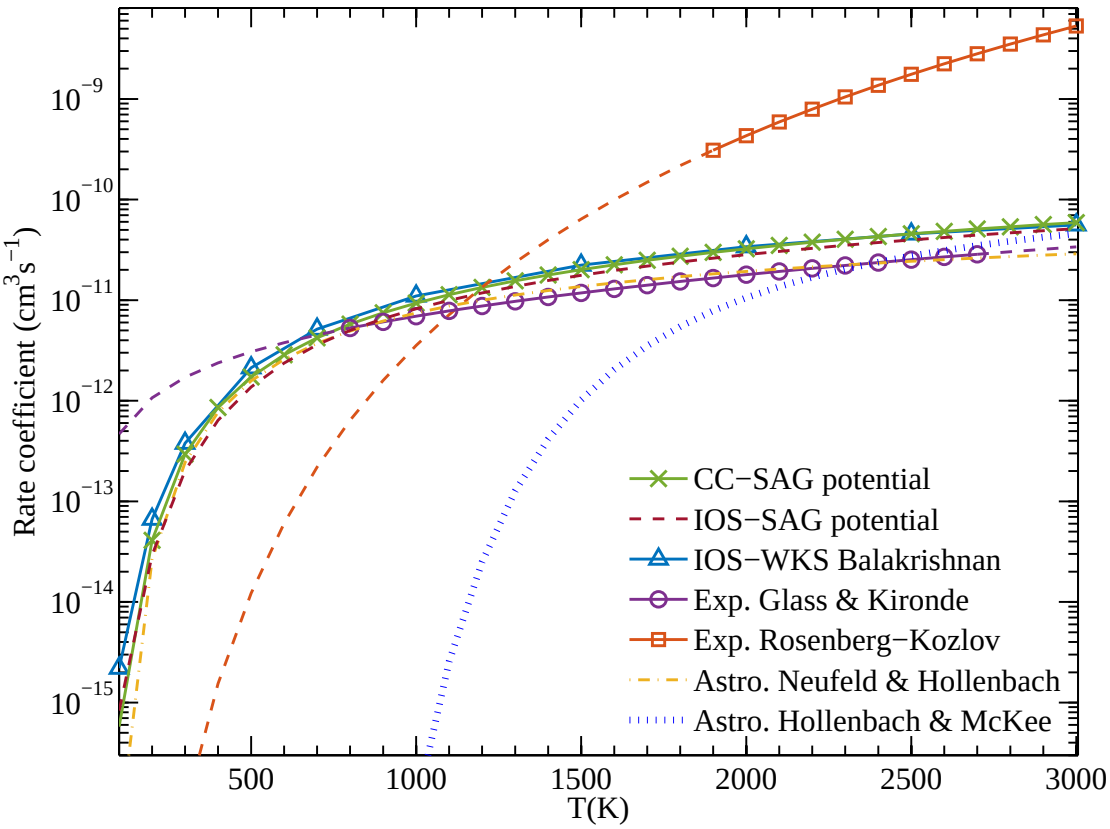

Figure 7. Comparison of vibrational $v = 1 \rightarrow v' = 0$ de-excitation rate coefficients of CO by collision with hydrogen atoms from different calculations and measurements.

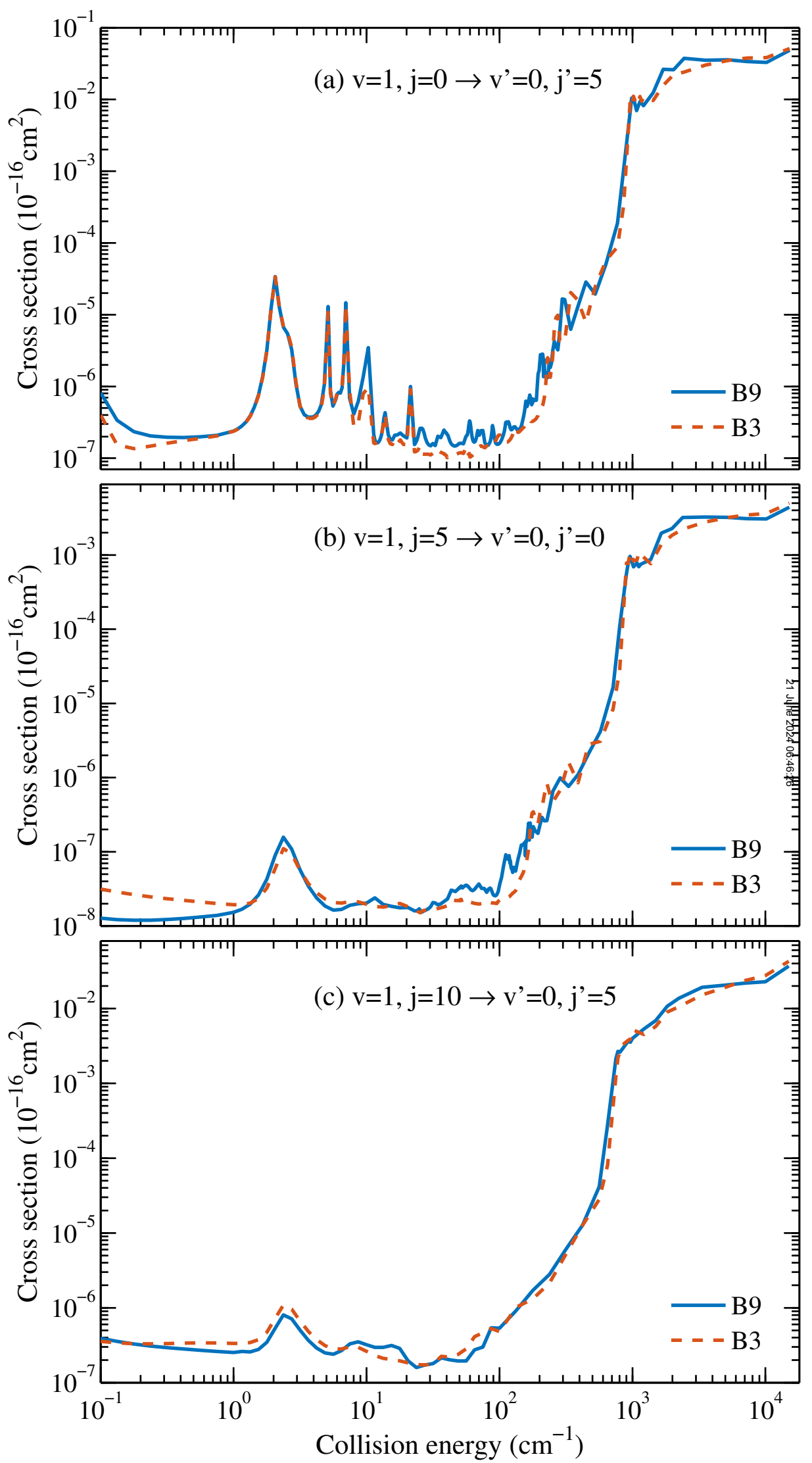
(a) v=1, j=0 → v'=0, j'=5
(b) v=1, j=5 → v'=0, j'=0
(c) v=1, j=10 → v'=0, j'=5
Cross section (10^{-16}cm^2)
Collision energy (cm^{-1})
B9
B3
21 June 2024 06:46:48

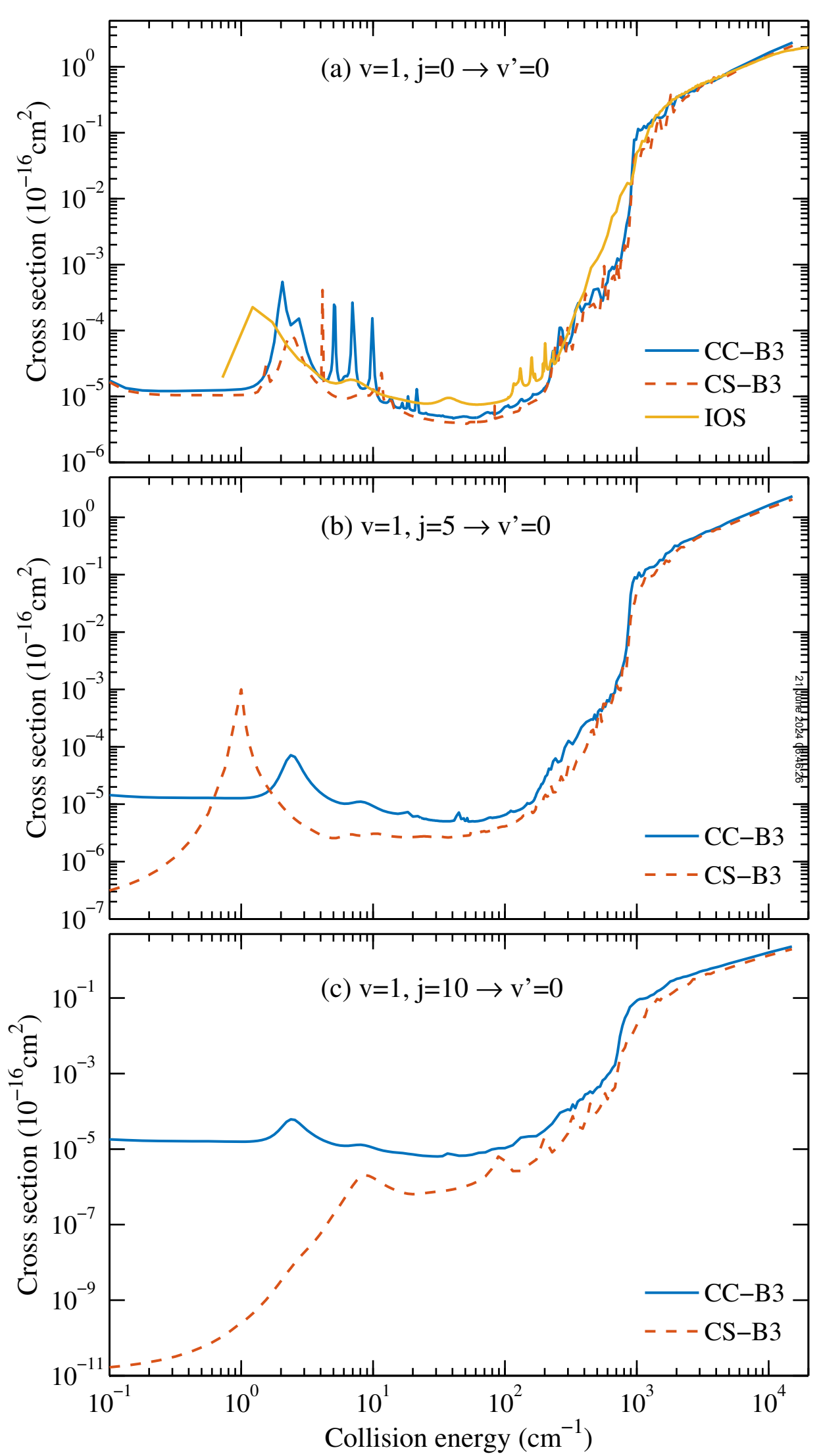
(a) v=1, j=0 → v'=0
Cross section (10^{-16}cm^2)
CC–B3
CS–B3
IOS
(b) v=1, j=5 → v'=0
Cross section (10^{-16}cm^2)
CC–B3
CS–B3
(c) v=1, j=10 → v'=0
Cross section (10^{-16}cm^2)
CC–B3
CS–B3
Collision energy (cm^{-1})

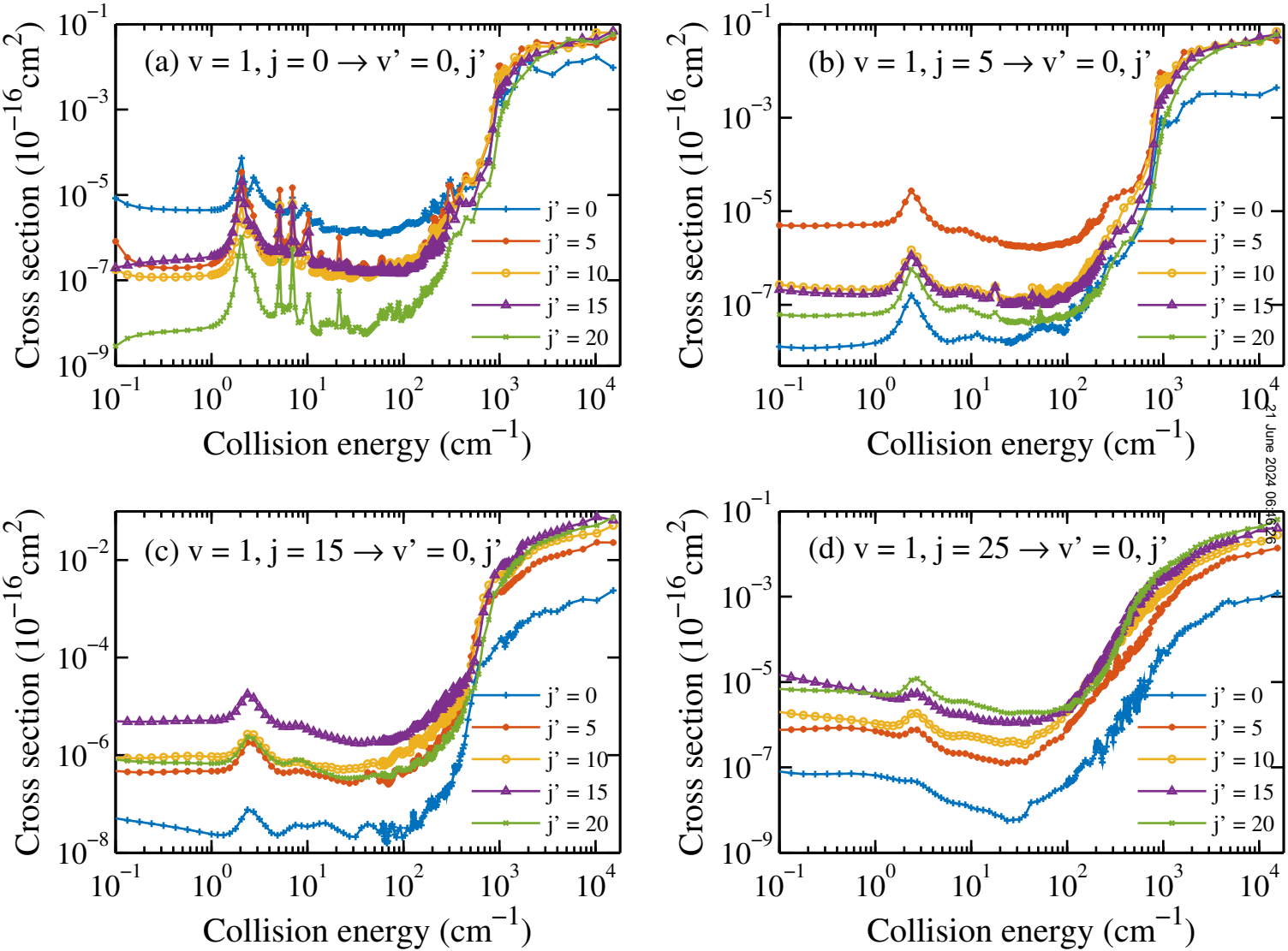

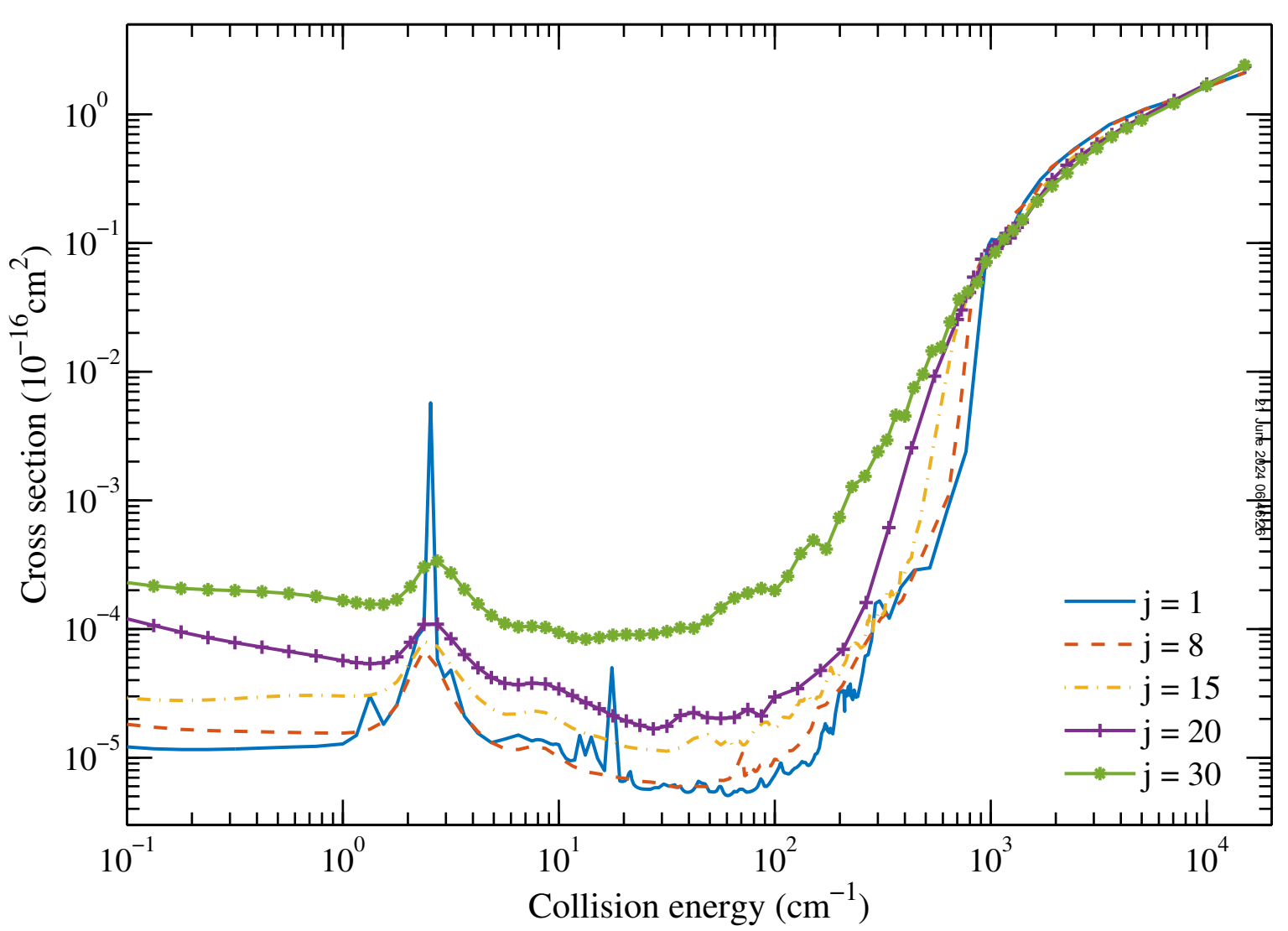
Cross section (10^{-16}cm^2)
10^{0}
10^{-1}
10^{-2}
10^{-3}
10^{-4}
10^{-5}
10^{-1}
10^{0}
10^{1}
10^{2}
10^{3}
10^{4}
Collision energy (cm^{-1})
j = 1
j = 8
j = 15
j = 20
j = 30
21 June 2024 06:18:26

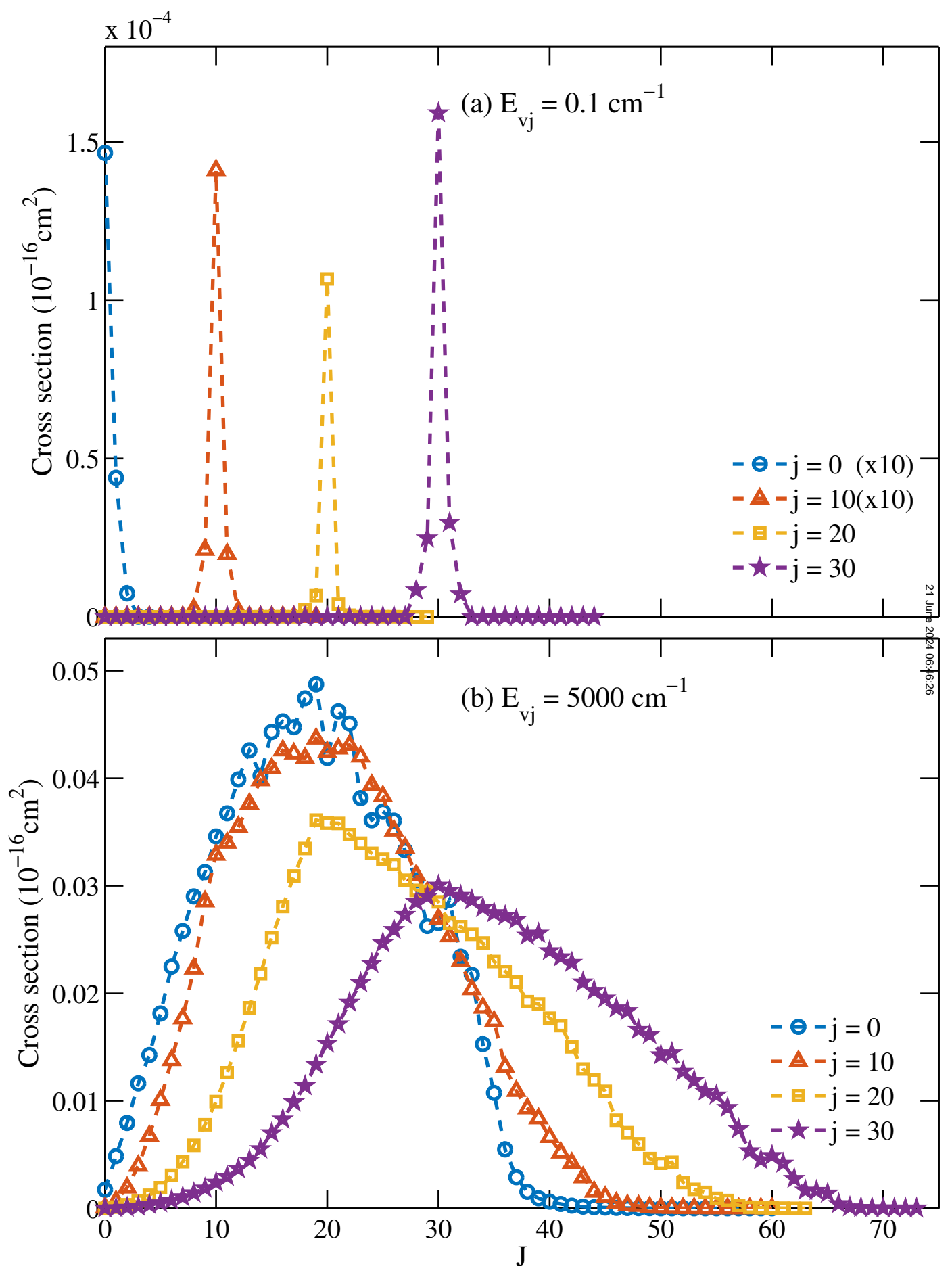
x 10^-4
(a) E_vj = 0.1 cm^-1
Cross section (10^-16 cm^2)
1.5
1
0.5
0
j = 0 (x10)
j = 10(x10)
j = 20
j = 30
21 June 2024 06:46:26
(b) E_vj = 5000 cm^-1
Cross section (10^-16 cm^2)
0.05
0.04
0.03
0.02
0.01
0
j = 0
j = 10
j = 20
j = 30
0
10
20
30
40
50
60
70
J

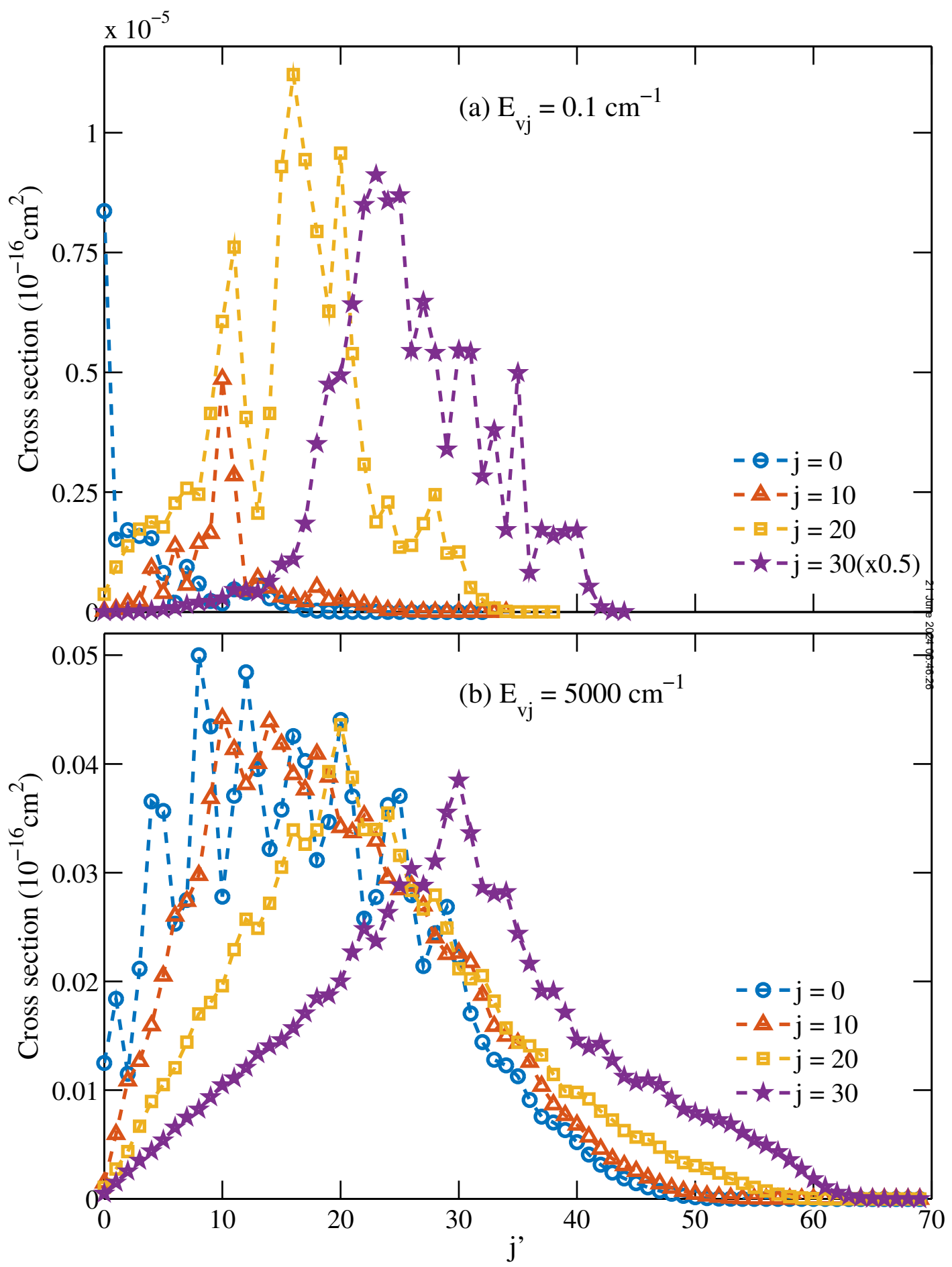
x 10^-5
(a) E_vj = 0.1 cm^-1
Cross section (10^-16 cm^2)
1
0.75
0.5
0.25
0
j = 0
j = 10
j = 20
j = 30(x0.5)
(b) E_vj = 5000 cm^-1
Cross section (10^-16 cm^2)
0.05
0.04
0.03
0.02
0.01
0
j = 0
j = 10
j = 20
j = 30
0
10
20
30
40
50
60
70
j'

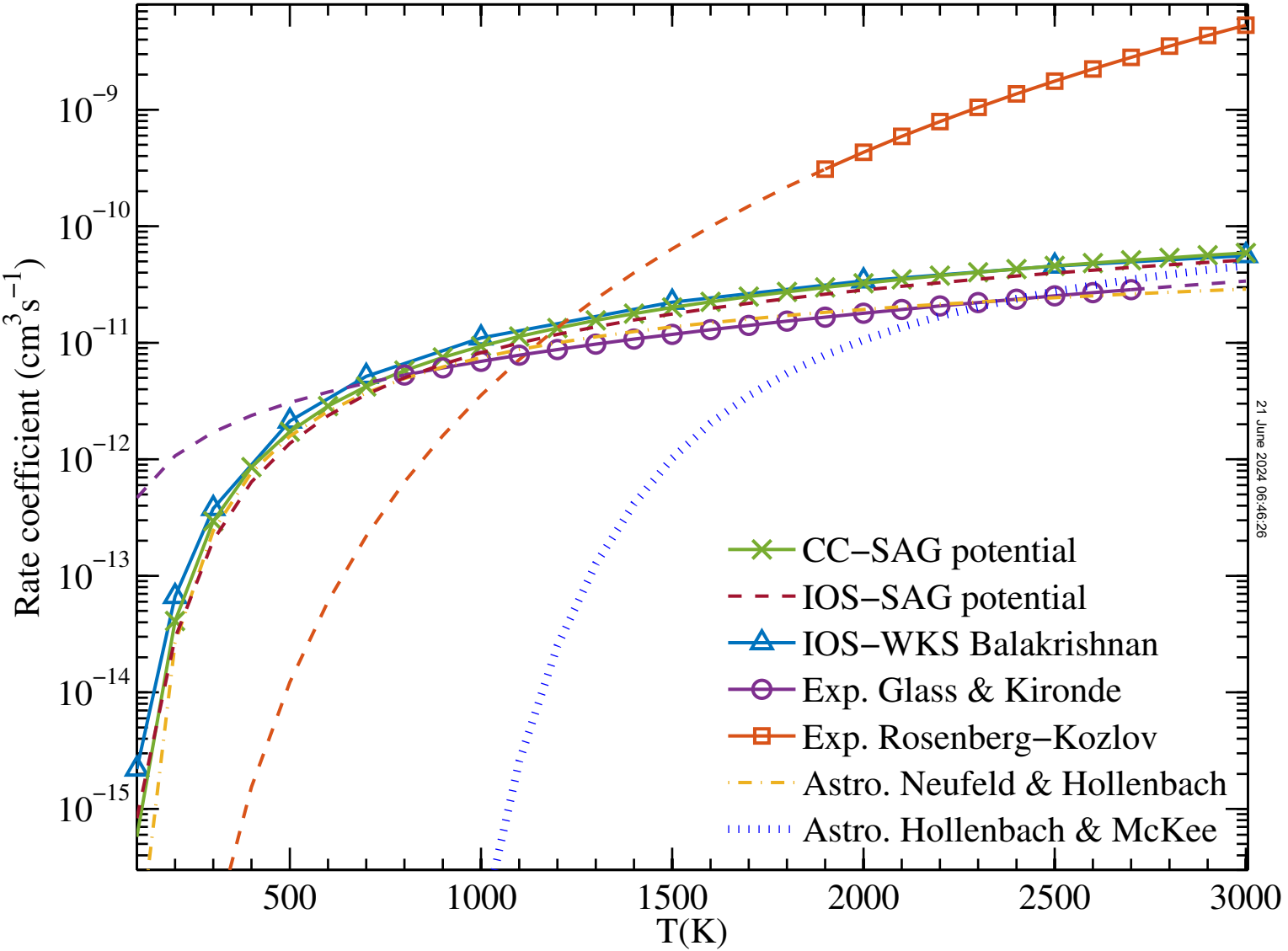
Rate coefficient (cm^3 s^{-1})
10^{-9}
10^{-10}
10^{-11}
10^{-12}
10^{-13}
10^{-14}
10^{-15}
500
1000
1500
2000
2500
3000
T(K)
CC−SAG potential
IOS−SAG potential
IOS−WKS Balakrishnan
Exp. Glass & Kironde
Exp. Rosenberg−Kozlov
Astro. Neufeld & Hollenbach
Astro. Hollenbach & McKee
21 June 2024 06:46:26